

Spatially-resolved local galaxies with multi-filter surveys: A 2-D study of the ALHAMBRA galaxies

I. San Roman¹, A. J. Cenarro¹, L. A. Díaz-García¹, C. López-Sanjuan¹, J. Varela¹ and the ALHAMBRA collaboration

¹ Centro de Estudios de Física del Cosmos de Aragón (CEFCA), Plaza San Juan 1, E-44001 Teruel, Spain

Abstract

We have developed a new technique using a novel approach to analyze unresolved stellar populations of spatially-resolved galaxies based on photometric multi-filter surveys. We have derived spatially resolved stellar population properties and radial gradients by applying a Centroidal Voronoi Tessellation and performing a multi-color photometry SED fitting. This technique has been successfully applied to a representative sample of 30 massive, early-type galaxies at $z < 0.3$ from the ALHAMBRA survey. Luminosity-weighted and mass-weighted gradients have been derived out to $2 - 3.5 R_{\text{eff}}$. We find the gradients of early-type galaxies to be on average flat in age ($\nabla \log \text{Age}_L = 0.02 \pm 0.18 \text{ dex } R_{\text{eff}}^{-1}$) and negative in metallicity ($\nabla [\text{Fe}/\text{H}]_L = -0.15 \pm 0.16 \text{ dex } R_{\text{eff}}^{-1}$). These results are in agreement with previous studies that used standard long-slit spectroscopy as well as with the most recent IFU studies. According to recent simulations, these results are consistent with a scenario where early-type galaxies have formed through major mergers. In this study, we demonstrate the scientific potential of multi-filter photometry to explore the spatially-resolved stellar populations of local galaxies and confirm previous spectroscopic trends from a complementary approach.

1 Introduction

Internal inhomogeneities of a galaxy, as radial age and metallicity gradients, are the results of its star formation and enrichment history. Therefore, spatially studies of galaxies are essential to uncover the formation and evolution of local galaxies. The arrival of integral field spectroscopy (IFS) have brought a significant breakthrough in the field. These IFS surveys allow detailed internal analysis through multiple spectra of each galaxy performing a 2D map of the object. The conclusions of these diversity of IFU as well as standard long-slit spectroscopy studies are not fully consistent so more detailed observational data containing spatial information are required to further constrain the formation history and the different mechanisms involved in the assembly of galaxies.

Currently, the number of multi-filter surveys is significantly increasing (e.g. J-PAS [1]). Half-way between classical photometry and spectroscopy, these surveys will build a formidable legacy data set by delivering low resolution spectroscopy for every pixel over a large area of the sky. It is clear that multi-filter surveys open a way to improve our knowledge of galaxy formation and evolution complementing standard multi-object spectroscopy surveys. To fully exploit the capabilities of multi-filter surveys, we have implemented a new technique that combine multi-filter SED fitting codes with an adequate spatial binning. In order to prove and test the reliability of our method we present a 2D analysis of the stellar population of early-type galaxy using the ALHAMBRA survey [6].

2 The method

The ALHAMBRA survey is a multi-filter survey carried out with the 3.5m telescope in the Calar Alto Observatory (CAHA) using the wide-field optical camera LAICA and the near-infrared instrument Omega-2000. With 20 contiguous, medium-band (FWHM $\sim 300 \text{ \AA}$) in the optical range and 3 broad-band filters in the near-infrared, ALHAMBRA survey covers a wavelength range between $\lambda 3500\text{--}9700 \text{ \AA}$ and spans a total area of 4 deg^2 over 8 non-contiguous regions of the northern hemisphere. In this work, we focus only in the analysis of early-type galaxies (spheroidal galaxies). In order to properly bin each galaxy, we also required a minimum apparent size of every object based on the isophotal aperture area. Additionally, galaxies with an insufficient signal-to-noise (S/N) to provide a reasonable 2D map were regretted. These selection provide us with a final sample of 30 massive, early-type galaxies at $z < 0.3$. The method used in the analysis can be resume in three main steps: the homogenization of the PSF, the spatially binning of each object, and the determination of the different stellar populations through the SED fitting of each bin to finally obtain the 2D maps.

Variations in the PSF from filter to filter will produce inhomogeneous photometry. To avoid this problem, we have developed a method to analyze, characterize and homogenize the PSF. This process will bring all images to the same, circular PSF, using variable PSF models and will ensure a homogeneous photometry. After the PSF homogenization is performed, an adequate spatial binning is required. We use the Centroidal Voronoi Tessellation (CVT) as the optimal binning technique where the size of the bin is adapted to the local S/N (e.g. bigger bins are applied in the low-S/N regions, while a higher resolution are retained in the higher-S/N parts). After the CVT has been performed, and the photometry of every bin in every filter was determined, we run the code MUFFIT [3] in every bin of the tessellation to obtain 2D maps of different stellar populations properties. The code compares the multi-filter fluxes of galaxies with the synthetic photometry of mixtures of two single stellar populations (SSP) at different redshifts and extinctions through an error-weighted χ^2 approach. We provides MUFFIT with two different types of SSP models as input set of models, BC03 [2] and MIUSCAT [7].

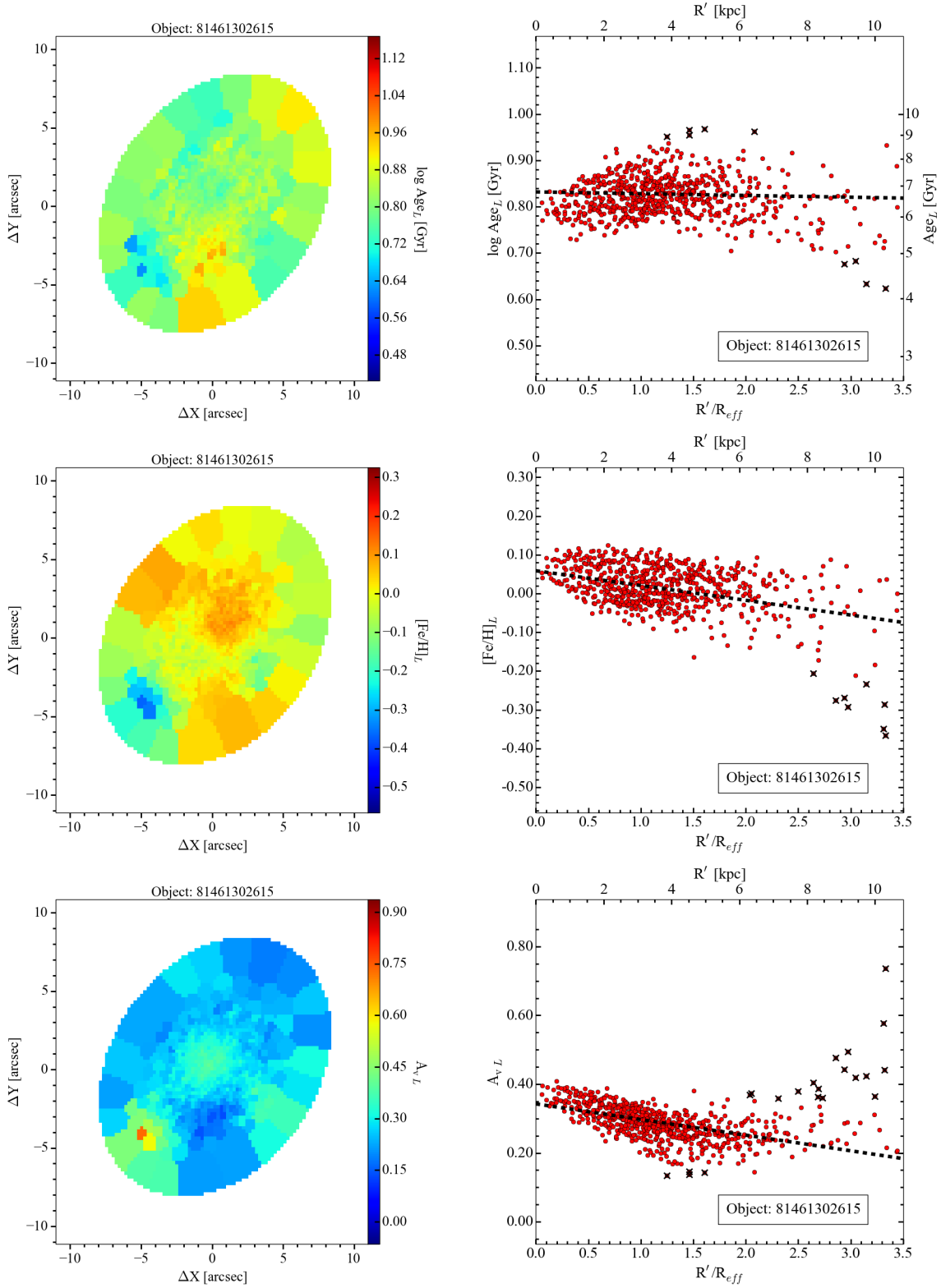


Figure 1: Luminosity-weighted stellar population properties maps and radial profiles analyzed using MIUSCAT-based models for the example object 81461302615. *Left column:* 2D maps for $\log \text{Age}$, $[\text{Fe}/\text{H}]$ and A_v covering an area of $22'' \times 22''$ around the target galaxy. The color range has been chosen to highlight inhomogeneities. *Right column:* $\log \text{Age}$, $[\text{Fe}/\text{H}]$ and A_v as a function of the circularized galactocentric distance R' . Each red circle symbol corresponds to a bin in the 2D map. Black dashed line corresponds to the error-weighted linear fitting. Black crosses represent values not considered during the fit.

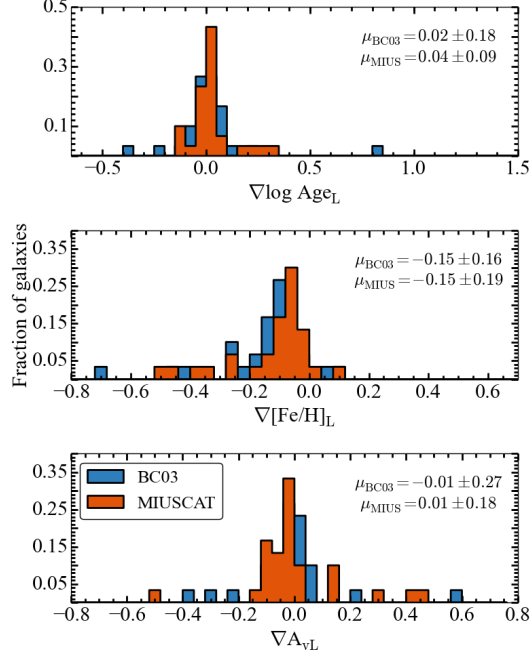


Figure 2: Histograms of the gradients for $\log \text{Age}_L$ (upper panel), $[\text{Fe}/\text{H}]_L$ (middle panel) and $A_{V,L}$ (bottom panel) for different SSP models.

3 Radial profiles and gradients

MUFFIT provides both luminosity and mass weighted ages, metallicities and extinctions. To show and quantify radial variations of the galaxies, we obtain the radial profiles of the three parameters for all the 30 galaxies. Radial profiles are obtained by plotting the stellar population values of each bin in each object as a function of the circularized galactocentric distance, R' . As an illustrative example, Fig. 1 presents the age, metallicity and extinction maps and radial profiles of a galaxy using MIUSCAT models and luminosity-weighted properties. Radial gradients were determined through an error-weighted linear fitting of the profiles out to 2–3.5 R_{eff} . The process was done iteratively via a sigma clipping on the residuals to remove outliers.

The age, metallicity and extinction light-weighted gradients for our sample are summarized in the histograms of Fig. 2. Our sample of early-type galaxies has, on average, a flat or slightly positive age gradients with a mean of $\nabla \log \text{Age}_L = 0.02 \pm 0.18 \text{ dex } R_{\text{eff}}^{-1}$ and $\nabla \log \text{Age}_L = 0.04 \pm 0.09 \text{ dex } R_{\text{eff}}^{-1}$ for BC03 and MIUSCAT respectively. These results agree very well with previous analysis of early-type galaxies as well as with the most recent IFU studies, in particular regarding the lack of a significant age gradient. The vast majority of our galaxies have negative metallicity gradients as expected in most of the galaxy formation

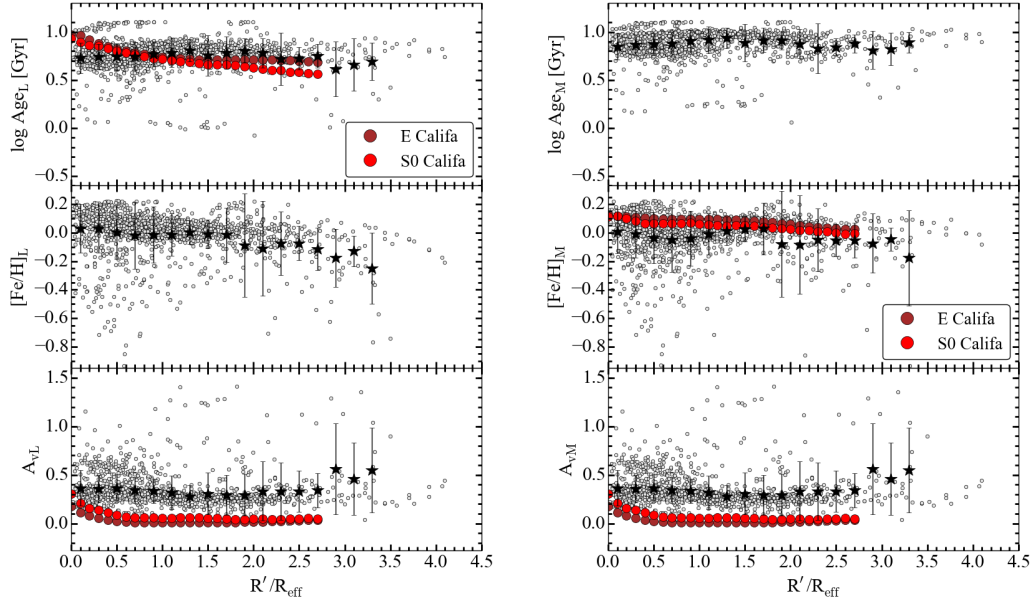


Figure 3: Stacked radial profiles of $\log \text{Age}$, $[\text{Fe}/\text{H}]$ and A_v for the case of MIUSCAT SSP models. Gray open symbols correspond to the stellar population values of each individual bin in each spatially resolved object. Star symbols have been obtained by averaging the stellar population values of the sample in constant bins of $0.2 R_{\text{eff}}$ between $0 \leq R \leq 3.6 R_{\text{eff}}$. The error bars are the standard deviation of the mean. When available, the profiles obtained by CALIFA [4] have been overplotted.

scenarios. The mean gradients of our sample are $\nabla[\text{Fe}/\text{H}]/R_{\text{eff}} = -0.15 \pm 0.16 \text{ dex } R_{\text{eff}}^{-1}$ for BC03 and $\nabla[\text{Fe}/\text{H}]/R_{\text{eff}} = -0.15 \pm 0.19 \text{ dex } R_{\text{eff}}^{-1}$ for MIUSCAT. Although the use of different metallicity indicators makes direct comparison more difficult, our results are compatible with previous studies. No clear correlation between total stellar mass and stellar population gradients has been found in agreement with previous studies.

4 Discussion

Figure 3 shows the age, metallicity and extinction radial profiles obtained by stacking all the galaxies obtaining a master profile. The radial profiles of the three stellar population properties between both studies are remarkably similar considering the distinct methodology and technique used. Overall, the ALHAMBRA stellar ages show flat profiles. Still, the inner ($< 1 R_{\text{eff}}$) regions tend to be slightly ($\sim 1 \text{ Gyr}$) younger than intermediate ($1 < R_{\text{eff}} < 2$) regions. CALIFA galaxies show a slightly more negative profiles, specially inside the first R_{eff} . The stellar metallicities profiles show slightly declining profiles at all radii. A small offset appears between both studies inside the first $1.5 R_{\text{eff}}$ where CALIFA galaxies seem to be more

metal-rich. The existence of intrinsic systematic differences between the two methods seems to be the most plausible reason for the different absolute values of the derived properties. The discrepancies between the analysis of spectral features versus colors and the different SSP models used may be the main responsible for the offsets. The ALHAMBRA profiles are less well constrain beyond $2 R_{\text{eff}}$ showing a larger standard deviation. A larger sample and deeper photometry is needed for further analysis at larger galactocentric distances. The stellar extinction behavior of the galaxies in our sample is consistent with a flat profile suggesting no significant changes in the dust content of early-type galaxies showing a constant $A_v = 0.3$ mag at any given radius. In contrast, E and S0 CALIFA galaxies show negative A_v gradients until $R = 0.5 R_{\text{eff}}$ with a dust-free behavior at larger distances. In general, the behavior of the radial variation of the different stellar population is remarkably similar between the IFU CALIFA survey and our multi-filter ALHAMBRA study in spite of the difference technique used. These results highlight the scientific power of our 2D multi-filter methodology.

With a mean metallicity gradient of $\nabla[\text{Fe}/\text{H}]_{\text{L}} = -0.3 \pm 0.3 \text{ dex dex}^{-1}$, in log space, our study is compatible with the predictions of [5] of galaxies that have undergone major-mergers. However, the significant dispersion amongst the mean value is indicative of galaxy-to-galaxy differences. Age gradients, in these simulations, are in general mildly positive ($\langle \nabla \log \text{Age} \rangle = 0.04 \text{ dex dex}^{-1}$) due to older ages of the accreted stellar population than that of the in-situ formed stellar component. According to recent theoretical studies, our shallow negative metallicity and flat age gradients suggest that the early-type galaxies in our sample have formed through major mergers where the gradients are driven by the higher metallicity and the older age of the accreted stars, together with the different mixing behavior.

Acknowledgments

This work has been partially funded by the Spanish Ministerio de Ciencia e Innovación through the PNAYA, under the grant AYA2015-66211-C2-1-P. We also acknowledge financial support from the Aragón Government through the Research Group E103.

References

- [1] Benitez, N. et al., 2014, eprint arXiv:1403.5237
- [2] Bruzual, G., & Charlot S., 2003, MNRAS, 344, 1000
- [3] Díaz-García, L. A. et al., 2015, A&A, 582, A14
- [4] González Delgado, R. M. et al., 2014, A&A, 562, A47
- [5] Hirschmann, et al, 2015, MNRAS, 449, 528
- [6] Moles, M. et al., 2008, AJ, 136, 1325
- [7] Vazdekis, A. et al., 2012, MNRAS, 424, 157